AN EXPERIMENTAL STUDY ON STIFFNESS AND DAMPING OF AIR BEARING SLIDERS

Q. H. Zeng[1] and D. B. Bogy
Computer Mechanics Laboratory
Department of Mechanical Engineering
University of California
Berkeley, CA 94720

Abstract

The system identification method was applied to experimentally investigate the dynamic characteristics of air bearing sliders. The dynamic responses of sliders were measured, and the modal frequencies and damping ratios that are directly related to the stiffness and damping of the bearings were obtained by data processing and parameter identification. First, an experimental system was set up, and then a program was developed for data preprocessing and parameter estimation. The dynamic properties of two sliders (Types A and B) were investigated. It was found that they have quite different properties, and that the suspensions (flexure) significantly affect the modal frequencies and damping ratios of the air bearings, and thereby the dynamics characteristics of the air bearings. The preliminary results also show the proposed method is robust for experimentally evaluating the dynamic properties of slider-air bearings.

[1] Visiting researcher, Associate professor, Institute of Vibration Engineering, Nanjing University of Aeronautics & Astronautics, Nanjing, China.

1 Introduction

The dynamics characteristics of slider-air bearings are important issues for lower and more stable flying heights, faster slider settling, and more reliable slider-disk interfaces to further improve the performance of hard disk drives. As flying heights continue to decrease, it is essential for the slider's fluctuations, induced by the impacts of the slider and the disk's asperites, to be rapidly damped out so that the successive impacts will not drive the slider's motion into resonance and result in a crash. Tian et al. (1997) showed that flying height fluctuation can thermally induce an MR signal disturbance even when no actual head/disk contact occurs in the process. Recent simulation results (Zhang and Bogy, 1997) demonstrate that the heat flux variation between a slider and disk is directly related to the flying height fluctuation of the slider. Therefore controlling the fluctuation is also important for sliders with MR elements. The transient fluctuation is directly related to the dynamics properties of the slider-air bearings. Therefore, the evaluation of the dynamics properties, such as stiffness and damping, of the air-bearings becomes an important concern.

There are many analysis and simulation results available on the dynamics characteristics of slider air bearings, such as those works presented by Ono (1975), Smith and Iwan (1991), Hu and Bogy (1996). Recently, the modal analysis method (Zeng, et al. 1997) was proposed for analyzing the dynamics properties of slider-air bearings, and the method was shown to be a versatile tool for head-medium interface analysis. The dynamics properties of typical slider designs were evaluated by using the modal parameters, and new designs with high damping were presented by Zeng and Bogy (1997). Experimental techniques have also been applied to study the slider-disk interface to obtain the dynamics characteristics. For example, the effect of surface roughness and disk material on the dynamics of a slider was studied by using measured acoustic emission and vibration signals, but only qualitative damping results were presented (Suzuki and Nishihira, 1995).

Yura, et al.(1991) investigated the dynamic response of 50% sliders to a step on a disk. They identified the resonance of the air bearings, but their frequencies and damping ratios were not obtained. Hayashi and Ohkubo (1991) compared numerical and perturbation solution responses of sliders to bumps with the responses measured by a laser interferometer. The comparison method does not yield results that are convenient for applications. Therefore, it is necessary to investigate a systematic method to experimentally evaluate the dynamic characteristics of slider-air bearings.

In this report, we apply the system identification method to experimentally investigate the dynamics characteristics of air bearings. The dynamic responses of the sliders are measured. The modal frequencies and damping ratios that are directly related to the stiffness and damping of the bearings are obtained by data processing and parameter estimation. An experimental system was set up, and a program was developed for data preprocessing and parameter estimation. The dynamics properties of two advanced air bearing (AAB) sliders (Types A and B) were investigated. It was found that these two sliders have quite different properties, and that the suspensions (flexures) significantly affect the modal frequencies and damping ratios of the air bearings, and thereby the dynamic characteristics of the air bearings. The preliminary results also show the proposed method is robust for experimentally evaluating the dynamics properties of air bearing sliders.

2 Methods Of Parameter Estimation And Data Preprocessing

2.1 Basic idea and equations

Assuming the suspension-slider-air bearing system is linear, time-invariant, self-adjoint, and with viscous damping, the slider is a rigid body and vibrates in the range near its steady flying state, we can identify all dynamic parameters of the system if we can apply artificial excitations and can measure both the excitations and the responses of the system. Simulation results show that the modal frequencies of most slider-air bearings are between

30 kHz and 200 kHz (Zeng and Bogy, 1997). It is too difficult to apply a measurable artificial excitation for such a small system in this frequency range. It is well known that the modal frequencies and damping ratios of linear systems can be identified from free response data (the response for nonzero initial conditions). Transient data is widely used to determine the frequencies and damping ratios. In this report, we use the measured responses of the sliders to bumps on the disks to identify these quantities.

We can express the governing equations of the assumed restricted motion of the slider as (Zeng and Bogy, 1997)

$$[M]\{\ddot{u}\}+[C]\{\dot{u}\}+[K]\{u\}=\{f(t)\} \tag{1}$$

where [*M*], [*K*] and [*C*] are the mass, stiffness and damping matrices (3x3), $\{u\}=\{z, \theta, \beta\}^T$ is the vibration displacement vector of the slider, and z, θ and β are the slider's vertical displacement (from the steady flying condition) at the slider's center, and its pitch and roll. $\{f(t)\}$ is the external excitation force vector. After the sliders fly past the bump, we can assume that there is no external excitation ,i.e. $\{f(t)\}=0$, but the sliders continue to have a transient vibration displacement and velocity. The system is assumed to have three modes, and then its responses can be written as

$$h(t)=\sum_{r=1}^{3}\left(A_r e^{s_r t}+A_r^* e^{s_r^* t}\right) \tag{2}$$

where A_r is the modal participation factor (a complex constant), and

$$s_r=-2\pi f_r\xi_r+i2\pi f_r\sqrt{1-\xi_r^2}, r=1,2,3 \tag{3}$$

where ξ_r and f_r are the damping ratio and frequency of mode r.

2.2 Parameter estimation

If a measured response of the slider is $h(l\Delta t)$, $l=0,1,\ldots L$, and the sample interval is Δt, we can estimate the modal frequencies and damping ratios in the time domain or frequency domain. In the time domain, directly estimating s_r from Eq.(2) will encounter some

difficulties because of the non-linear relationship between s_r and $h(t)$. Therefore, the complex exponential method (Brown et al., 1979) is adopted. Assuming

$$x_r = \mathrm{e}^{s_r \Delta t} \tag{4}$$

based on Eq.(2), we can write the measured response of the N degree-of-freedom (DOF) system as

$$h(l\Delta t) = \mathrm{Re}\left(\sum_{r=1}^{2N} A_r x_r^l \right),\ l=0,1,2,\ \ldots,\ L. \tag{5}$$

We introduce a new set of real unknown parameters α_j ($j=0,1,\ldots,2N$) which are the coefficients of the terms in the polynomial equation

$$\sum_{j=0}^{2N} \alpha_j y^j = 0 \tag{6}$$

Replacing l in Eq.(5) by $l+j$, suppressing the Δt in the expression $h(l\Delta t)$, multiplying Eq. (5) by coefficients α_j, and adding all of the resultant equations ($j=0,1,\ldots,2N$), we can obtain

$$\sum_{j=0}^{2N} \alpha_j h(l+j) = \mathrm{Re}\left(\sum_{r=1}^{2N} A_r x_r^l \left(\sum_{j=0}^{2N} \alpha_j x_r^j \right) \right),\ l=0,1,\ldots,L \tag{7}$$

If the 2N solutions of Eq. (6) are x_r $(r=1,2,\ldots,2N)$, then equation (7) becomes

$$\sum_{j=0}^{2N} \alpha_j h(l+j) = 0,\ l=0,1,\ldots L. \tag{8}$$

Assuming $\alpha_{2N}=1$, one can construct the linear equation

$$\begin{bmatrix} h(0) & h(1) & \ldots & h(2N-1) \\ h(1) & h(2) & \ldots & h(2N) \\ \ldots & \ldots & \ldots & \ldots \\ h(L) & h(L+1) & \ldots & h(L+2N-1) \end{bmatrix} \begin{Bmatrix} \alpha_0 \\ \alpha_1 \\ \vdots \\ \alpha_{2N-1} \end{Bmatrix} = \begin{Bmatrix} h(2N) \\ h(2N+1) \\ \vdots \\ h(2N+L) \end{Bmatrix} \tag{9}$$

There is noise in the measured responses, so as many data points as possible are preferred. When $L>2N$, the least square method is used to solve Eq.(9) to find α_j. Then solving Eq.(6), one can obtain x_r and thereby find the modal frequencies and damping ratios from Eqs.(4) and (3). If more than one record in the same operational state are available, then using each record, one can construct a linear equation that is similar to Eq.(9). Different α_j

may be found from the different records because of the effects of the noise. Therefore, it is recommended to use the least square method to obtain one set of α_j by simultaneously solving all of the linear equations.

In the time domain, the major difficulty is that estimating the parameters requires many modes to compensate for the noise in the measured data. Theoretically, N=3 is sufficient, but N> 20 is usually required. Therefore, the frequency domain method is preferred over the time domain method in some situations. Performing the Fourier transformation of Eq.(2), one obtains

$$H(\omega)=\sum_{r=1}^{3}\left[\frac{A_r}{(\mathrm{i}\omega-s_r)}-\frac{A_r^*}{(\mathrm{i}\omega-s_r^*)}\right] \tag{10}$$

Then, the orthogonal rational fractional polynomial method (Zeng et al., 1997) can be adopted to estimate the modal frequency f_r and the damping ratios ξ_r.

2.3 Data pre-processing

The measured bump responses of the sliders can not be directly used to estimate the parameters because of the poor signal-to-noise (SN) ratio in most situations. It is necessary to perform data pre-processing to improve the SN ratio before the data can be used in the parameter estimation. Figure 1 shows two typical measured bump responses. The responses can be divided into several stages. The first stage is the free flying response. The second is the response when the trailing edge of the slider flies over the bump. Its length is dependent on the relative speed and width of the bump. The third is the free response with a higher SN ratios. The last is the free response with a lower SN ratio. The third stage response is used to estimate the parameters. However, not only is the third stage response contaminated by the noise, but it is also difficult to divide the third and fourth stages. Therefore, the following procedures are proposed.

1) Data truncation

The data needed are the free responses of the sliders. So, only the responses of the sliders after they have past over the bumps are valid. For most cases, we only use the responses after the second peak of the absolute values of the data, as shown in Figure 1. The best way is to use an additional measurement channel to accurately determine the beginning points of the free responses.

2) Filtering in the time domain

For the excitations of the random disturbances and measurement noise, the measured response can be expressed as

$$h_m(t) = h(t) + n(t) \tag{11}$$

where *h(t)* is the true free response of the slider for the bump and *n(t)* is the random noise, in which the response to the random disturbances and the measurement noise are included. Assuming the response of the slider is not correlated with the noise, we can calculate the auto-correlation function of $h_m(t)$ as

$$\begin{aligned} R_{h_m h_m}(\tau) &= \int_0^\infty \left(\sum_{r=1}^{2N} A_r e^{s_r(t+\tau)} \sum_{k=1}^{2N} A_k e^{s_k t} \right) dt + R_{nn}(\tau) \\ &= \sum_{r=1}^{2N} \left\{ A_r e^{s_r \tau} \int_0^\infty \left(\sum_{k=1}^{2N} A_k e^{(s_k+s_r)t} \right) dt \right\} + R_{nn}(\tau) \end{aligned} \tag{12}$$

or

$$R_{h_m h_m}(\tau) = \sum_{r=1}^{2N} (B_r e^{s_r \tau}) + R_{nn}(\tau), \quad \tau \geq 0 \tag{13}$$

Where $R_{nn}(\tau)$ is the auto-correlation of the *n(t)* noise, and B_r is a constant. If *n(t)* is white noise, $R_{nn}(\tau)$ is the delta function. Then, the auto-correlation function of the measured response $h_m(t)$ can be written as

$$R_{h_m h_m}(t) = \sum_{r=1}^{2N} B_r e^{s_r t}, \quad t > 0 \tag{14}$$

Equation (14) is equivalent to Eq. (2). Therefore, we can calculate the auto-correlation function of the measured response to eliminate the uncorrelated noises, and directly use the functions to estimate the modal frequencies and damping ratios.

3) Exponential window

The true free responses of the sliders will be damped out rapidly, such that the SN ratios will be decreased quickly. It will be helpful to apply a non-uniform weight function to the data that will be used in the parameter estimation, and provided effects of the function can been analytically eliminated. An exponential function is very suitable for this purpose, such as

$$W(t) = e^{-\frac{t}{T_w}}, \quad t \geq 0 \tag{15}$$

where T_w is the coefficient of the window. After the window is applied, and if the estimated modal frequencies and damping ratios are f_{rw} ($\omega_{rw}=2\pi f_{rw}$) and ξ_{rw}, then one has

$$\begin{cases} \xi_r \omega_r + \dfrac{1}{T_w} = \xi_{rw}\omega_{rw} \\ \sqrt{1-\xi_r}\,\omega_r = \sqrt{1-\xi_{rw}}\,\omega_{rw} \end{cases} \tag{16}$$

Solving Eq.(16), we can obtain the frequency f_r and damping ratio ξ_r in which the effects of the window are removed as follows

$$\omega_r = \sqrt{\omega_r^{\,2} - 2\xi_r\omega_r / T_w + 1/T_w^{\,2}} \tag{17}$$

$$\xi_r = (\xi_{rw}\omega_{rw} - 1/T_w)/\omega_r \tag{18}$$

3 Applications

3.1 Experimental setup and procedure

The experimental setup includes a spin-stand, a two-beam Laser Doppler Vibrometer (LDV), a data acquisition system, and computer. We used the Lotus 7000 CSS tester as the spin-stand. It is convenient for adjusting the rotation speed of the disks, normal loads (or Z-height), and radial position of the sliders. The relative speed of 14.1 m/s (4000 RPM

at 33.7 mm radial position) was chosen. The Polytec OSF 1100 LDV was used to measure the velocity responses of the sliders. Sometimes, we used its two beams to measure the roll and pitch responses, and sometimes we used only one beam to measure the absolute responses of the sliders. The fast tracking filter of the LDV was always used to improve the SN ratios because the responses were usually very small. A Data 6000 digital recorder was used to acquire the responses. The sample interval was 0.2 μS, and the number of data points was 2048. The frequency range of the vibrations of the slider-air bearings for the most current 50% and 30% sliders is between 30 kHz and 200kHz. We were only interested in the slider-air bearing vibrations, so a band-pass filter with a pass band of 25 kHz to 300 kHz was added between the LDV and the Data 6000. A high pass filter is always necessary for measuring the absolute responses of the sliders because the signals of the disk vibration are very strong in the lower frequency band. A program was developed to read the data from the Data 6000 to the PC, and perform the data pre-processing and parameter estimation.

3.2 Experimental samples

A 3.5 inch disk was used in the experiments. The disk had 2 nm of Z-DOL lubricant, 17.5 nm of DLC overcoat, 4 nm rms roughness, and 3.5 nm waviness. The disk was scratched lightly by a sharp knife. The scratch mark was about 10 mm in length in the radial direction, and it was about 40 μm wide. The depth was between 100 nm and 300 nm, and the ridge heights of the two sides were between 50 nm and 80 nm. For our experiments, an accurate knowledge of the dimensions of the bumps is not necessary. What we required was that the sliders not impact with the bumps, and the bumps could induce sufficiently large fluctuations of the sliders.

Two types of the suspension assemblies, as shown in Figure 2, were used. The air bearing surfaces (ABS) of the two sliders are very similar and are also show in Figure 2. Both are

AAB (advanced air bearing) sliders with sub-ambient pressure regions. Type B has a step ABS. Its air bearing should have larger damping than Type A, based on our previous results (Zeng and Bogy, 1997). The load beams of the two suspension assemblies are similar, but their flexures are quite different (see Figure 3 and Figure 9). The flexure of Type A is a two-piece structure. Type B has a one-piece flexure.

3.3 Measured data and results for the Type A slider

There are eight measurement cases. The measurement points are shown in Figure 3. The measurement cases are shown in Table 1. Each case had ten measurement records. Figure 4 shows some measurement data. From the figure we can see that the measurement has very good repeatability. All of the measured raw data were processed by the proposed procedure, explained above.

Based on the simulation results, the system has three modes in the assumed restricted motion– one roll mode and two pitch modes. Cases 1 and 2 were mainly for measuring the roll motion. Almost the same results were obtained from the two cases. Figure 5 shows the raw data and processed results of one record. After the data processing, we obtained the pure response of a single mode. This mode must be the roll mode. No response component of the other two modes was found. That means the nodal lines of the two pitch modes are parallel to the leading and trailing edges. Cases 3 and 4 are for measuring the pitch motion. However, Figure 6 d) shows three peaks rather than two. They correspond to the two pitch modes and the roll mode. That means the nodal line of the roll mode is not parallel to the central line of the slider. Figure 7 shows the measured absolute velocity response at the corner of the leading edge and the outer rail. The two peaks in Figure 7 d) are the responses of the first pitch and roll modes. Figure 8 shows the measured absolute response at the center of the trailing edge. The two peaks in Figure 8 d) are responses of

the second pitch and roll modes. The results indicate that the nodal line of the roll mode does not pass through the center of the trailing edge.

After the data preprocessing, we made the parameter estimation by using both the time domain and frequency domain methods. The data of cases 3, 4, 5 and 6 were simultaneously used to estimate the first pitch mode (mode 1). The data of cases 3, 4, 5, 7 and 8 were simultaneously used to estimate the second pitch mode (mode 3). The data of cases 1, 2, 5, 6 and 7 were simultaneously used to estimate the roll mode (mode 2). The first 230 data points and 50 modes ($l=1,2,\ldots,230;\ N=50$ in Eq.(8)) were selected to estimate the three modes by using the time domain method. The modal frequencies and damping ratios are shown in Table 2. Similar results were obtained by using the frequency domain method. For comparison, the simulation results in which the effects of the suspension are not included are also show in the table. We can see that the modal frequencies obtained by the experiment and simulation are close to each other, but the experimental damping ratios are much lager than the simulation results. The large differences in the damping ratios are probably induced by the effects of the suspension. The errors in the experiments and simulation would also result in differences. We can not quantitatively estimate the errors of the experimental results, but it is believed that the measured frequency and damping ratios of the roll mode are very reliable.

3.4 Measured data and results of the Type B slider

There are six measurement cases. The measurement points are shown in Figure 9. The point D is located on the slider through the slit in the load beam. The measurement cases are shown in Table 3. Again, each case had ten measurement records. Figure 10 shows some measurement data. From the figure we can see that the repeatability of this measurement is also very good. Comparing Figure 10 with Figure 4, we can see that the

bump responses of the Type B slider take longer time to be damped out than for the Type A slider.

Cases 1 mainly measured the roll motion. Figure 11 shows the raw data and processed results of one record. After the data processing, we obtained the pure response of the single mode. This is the roll mode. We can not find any response of the other modes in this measurement. That means the nodal lines of the other modes are parallel to the trailing edge. Cases 2 measured the pitch motion. However, Figure 12 d) clearly shows three peaks. One of them has the frequency of about 25 kHz. Simulation results do not show any mode of the slider-air bearings in this frequency range. Figure 13 shows the measured absolute velocity response at the corner of the leading edge and the outer rail. There are also three peaks in Figure 13 d). Figure 14 shows the measured velocity absolute response at the center of the trailing edge. The beating phenomena shown in Figure 14 a) indicates that there are two modes with close frequency. Figure 14 d) shows these two frequencies are about 74 kHz and 83 kHz. We found more than three modes, and only the roll mode (at about 80 kHz) was identified. Figure 15 was used to identify the rest of the modes. The first pitch mode should have a large contribution to the responses in cases 2 and 5, and little contribution to the responses in cases 1 and 3. From Figure 15, it appears that the peak at about 43 kHz is the response of the first pitch mode. The second pitch mode should have a large contribution to the responses in case 2 and 3, and small contribution to cases 1 and 5. From the figure, it appears that the peak at about 84 kHz is the response of the second pitch mode. The remaining two peaks are the responses of additional modes with about 25 kHz and 73 kHz frequencies.

After the data preprocessing and identification of the modes, we made the parameter estimation. The data of cases 2, 5 and 6 were simultaneously used to estimate the first pitch mode (mode 1). The data of cases 2, 3 and 4 were simultaneously used to estimate

the second pitch mode (mode 3). The data of cases 1, 4 and 5 were simultaneously used to estimate the roll mode (mode 2). The modal frequencies and damping ratios are shown in Table 4. The experimental results for the Type A slider are also show in the table for easy comparison. We can see that the Type B slider has very different dynamic properties. Its air bearing has lower stiffness.

The simulation results show the ABS of the Type B slider should create an air bearing with larger damping than that of Type A. However, the experimental results shown the damping of the Type B slider is much smaller than that of Type A. It is probable that the effects of the suspensions result in the very different damping. The Type B slider has an integrated gimbal structure. Its damping is mainly from the material, giving damping that is very small. The Type A slider has a two-piece gimbal structure. Its damping is from the material and contact between the load beam and flexure. The contact between two surfaces ordinarily generates large damping. Such contact is a non-linear problem. If indeed it is the contact that provides the larger damping, then the contact will also introduce the non-linear properties. So, the experimental data should show the non-linear property. This possibility is examined next.

Figure 16 shows the processed roll responses and curve fits of the two sliders. The first 150 points (.03ms, the first band) were used to estimate the modal parameters in the time domain. The estimated parameters were used to generate the curve fits. We can see that the curve fits are very close to the processed data initially, and the differences between the data and the curve fits gradually increase with time or the decrease of the amplitude. The figure shows an important difference between Type A and Type B. Figure 16 a) shows a gradual phase shift between the data and the curve fit for Type A. That means the frequency of the roll mode is time-variant. Figure 16 b) shows no any phase shift of Type

B. That means the frequency of the roll mode is not time-variant, or is not dependent on the vibration amplitude.

To find the relationship between the modal parameters and the time, we used different data bands to estimate the parameters. Each band has the same width (.03 ms), and starts at a different peak as shown in Figure 16. Different modal parameters can be obtained from the different bands. Two records were analyzed for each type. The modal frequencies and damping ratios are shown in Figure 17. We can see that the modal frequency of Type A is dependent on the time or vibration amplitude, while the frequency of Type B is not dependent on them. Because the estimated damping ratios are more sensitive to the noise than the frequencies, consistent damping estimations can not been obtained in the range with smaller amplitudes. Thus, the experimental results shows that Type A exhibits the non-linear property and Type B is a linear system. It is believed that the contact between the loadbeam and the gimbal results in the non-linear property, and high damping of Type A, but other suspension related responses are also possible explanations. This will be studied further in future research.

4 Conclusions

We applied the system identification method to experimentally investigate the dynamic properties of slider-air bearings. A data preprocessing procedure was proposed to process the measured bump responses of the sliders. Both the time domain and frequency domain methods were used to estimate the modal frequencies and damping rations of the system.

The dynamic properties of two AAB sliders were investigated. It was found that they have quite different properties. The suspension (flexure) significantly affect the modal frequencies and damping ratios of the air bearings, and thereby the dynamic characteristics of the system. The two-piece suspensions provide more damping for the air bearing than the integrated suspensions.

The experimental results show that the proposed method is robust for experimentally evaluating the dynamic properties of slider-air bearings. The measured damping ratios are much larger than the simulation results in which the effects of suspensions are not included. More research is required to further confirm the results and model the effects of the suspensions on the air bearings.

ACKNOWLEDGMENTS

This study is supported by the Computer Mechanics Laboratory at the University of California at Berkeley and Quantum Corporation.

REFERENCES

Brown, D. L., Allemang, R. J., Zimmerman, R. and Mergeay, M., 1979,"Parameter Estimation Techniques for Modal Analysis," SAE 790221.

Hayashi, T. and Ohkubo, T., 1991, "Comparison of the Direct Numerical Solution and the Perturbation Solution in the Dynamic Analysis of a Flying Head Slider for Magnetic Disk Storage Operating at Very Low Spacing," *ASME, Adv. in Info. Storage Syst.*, Vol. 2, pp. 113-125.

Hu, Y. and Bogy, D. B., 1996, "Dynamics Stability and Spacing Modulation of Sub-25 nm Fly Height Sliders," *ASME, 96-Trib-56.*

Ono, K., 1975, "Dynamic Characteristics of Air-Lubricated Slider Bearing for Noncontact Magnetic Recording," *J. of Lubrication Technology*, 250-260.

Peck, P.R., Wang, B. S., Park, K.O. and Jhon, M. S., 1995, "Scaling Criteria for Slider Miniaturization Including Shape Effects," *Proc. Sixth Intl. Symp. Adv. Infr. Storage Proc. system*, ISPS-Vol. 1, 1-6.

Smith, P. W. and Iwan, W. D., 1991, "Dynamic Figures of Merit for the Design of Gas-Lubricated Slider Bearings," *ASME, Adv. in Info. Storage Syst.*, V.3, 41-53.

Suzuki, S., and Nishihira, H., 1995, "Study of Slider Dynamics over Very Smooth Magnetic Disks", *J. of Tribology* (95-Trib-38).

Tian, H., Cheung C.Y. and Wang, P.K., 1997, "Non-Contact Induced Thermal Disturbance of MR Head Signals," *Digests of INTERMAG'97*, AR-11.

Yura, S., Matsuura, T., Fujita, J. and Suzuki, S., 1991, "Dynamics Response of Flying Head Sliders to a Step on a Disk," *ASME, Adv. in Info. Storage Syst.*, Vol. 2, 103-111.

Zeng, Q.H., Chen. L.S. and Bogy, D.B., 1997, "A Modal Analysis Method for Slider Air Bearing in Hard Disk Drives," *Digests of INTERMAG'97*, AR-09, IEEE Tran.on Magnetics (submitted).

Zeng, Q.H. and Bogy, D.B., 1997, "Stiffness and Damping Evaluation of Air Bearing Sliders by Modal Analysis Methods: New Designs with High Damping," Technical Report No. 97-002, Computer Mechanics Lab., Dept. of Mechanical Engineering, University of California at Berkeley.

Zhang, S.Y. and Bogy, D.B., 1997, "Variation of the Heat Flux Between a Slider And the Air Bearing when the Slider Flies over an Asperity," Technical Report No. 97-0??, Computer Mechanics Lab., Dept. of Mechanical Engineering, University of California at Berkeley.

Case	Responses	Point	Modes which will mainly contribute to the responses
1	Relative	A-B	roll mode
2	Relative	C-D	roll mode
3	Relative	B-C	pitch modes
4	Relative	A-D	pitch modes
5	Relative	A-C	Pitch and roll modes
6	Absolute	C	1^{st} pitch and roll modes
7	Absolute	B	2^{nd} pitch and roll modes
8	Absolute	E	2^{nd} pitch mode

Table 1 Measurement cases – Type A

Mode	Shape	Simulation		Experiment	
		Freq. (kHz)	Damp.(%)	Freq.(kHz)	Damp.(%)
1	1st Pitch	49.11	3.05	45.65	12.1
2	Roll	102.2	0.91	94.00	3.65
3	2nd Pitch	105.9	1.11	114.2	5.40

Table 2 Modal frequencies and damping ratios - Type A

Case	Responses	Point	Modes which will mainly contribute to the response
1	Relative	A-B	roll mode
2	Relative	A-D	pitch modes
3	Absolute	A	2nd pitch mode
4	Absolute	B	2nd pitch and roll modes
5	Absolute	C	1st pitch and roll modes
6	Absolute	D	1st pitch mode

Table 3 Measurement cases – Type B

Mode	Shape	Type B		Type A	
		Freq. (kHz)	Damp.(%)	Freq.(kHz)	Damp.(%)
1	1st Pitch	43.05	3.08	45.65	12.1
2	Roll	80.39	2.55	94.00	3.65
3	2nd Pitch	83.50	2.26	115.1	5.40
Additional Modes		26.69	11.7		
		73.48	2.29		

Table 4 Measured modal frequencies and damping ratios

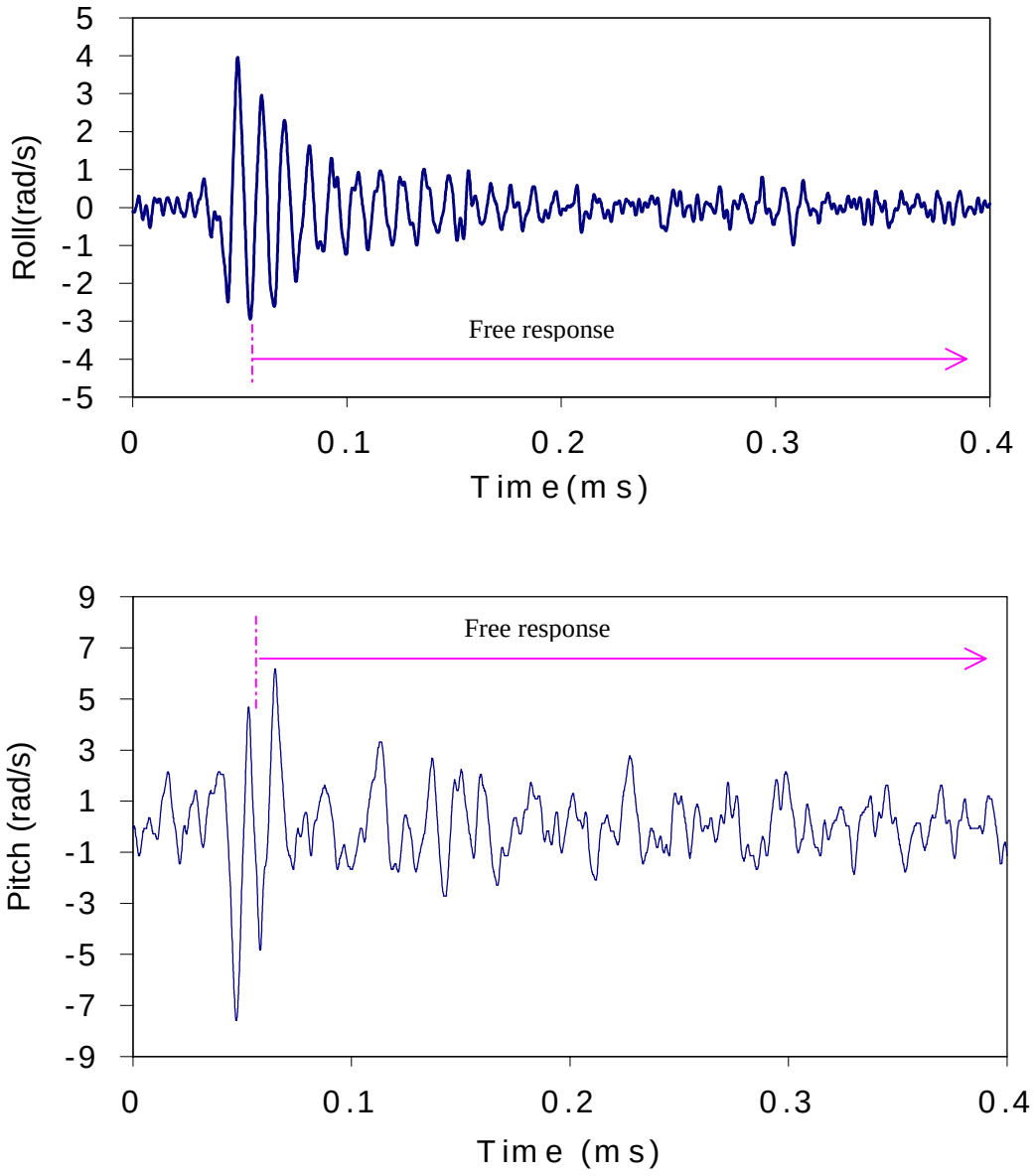

Figure 1 Two typical bump responses

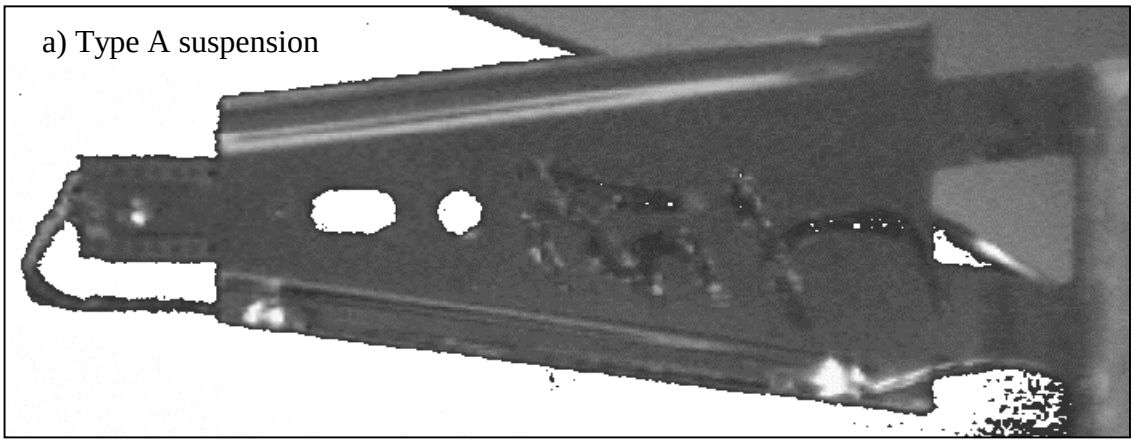

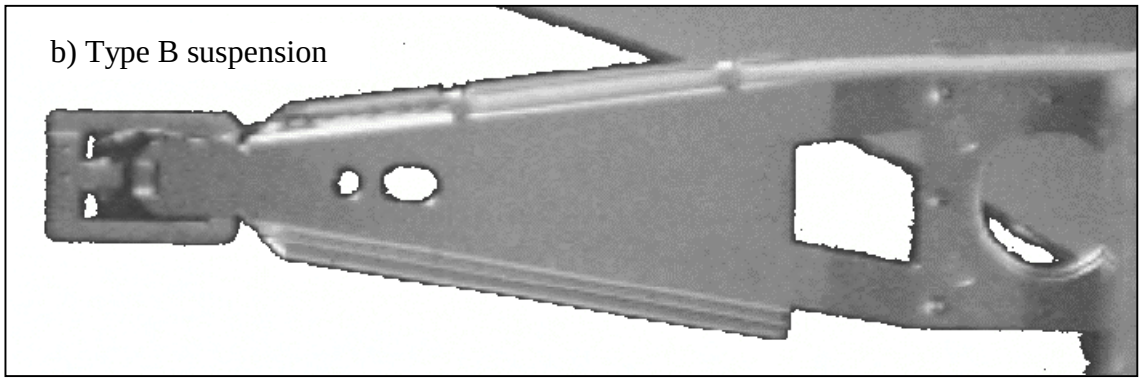

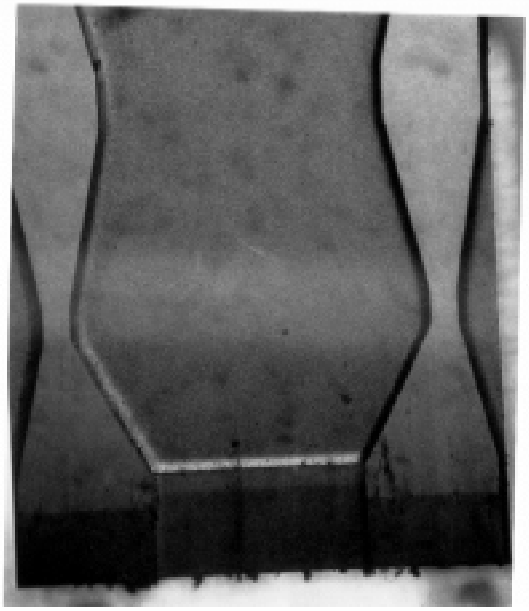

c) Type A ABS

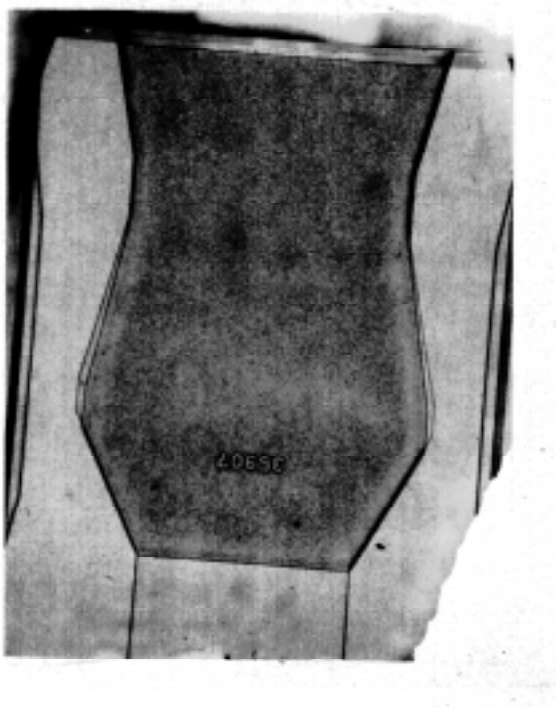

d) Type B ABS

Figure 2 Suspension assemblies and air bearing surfaces(ABS)

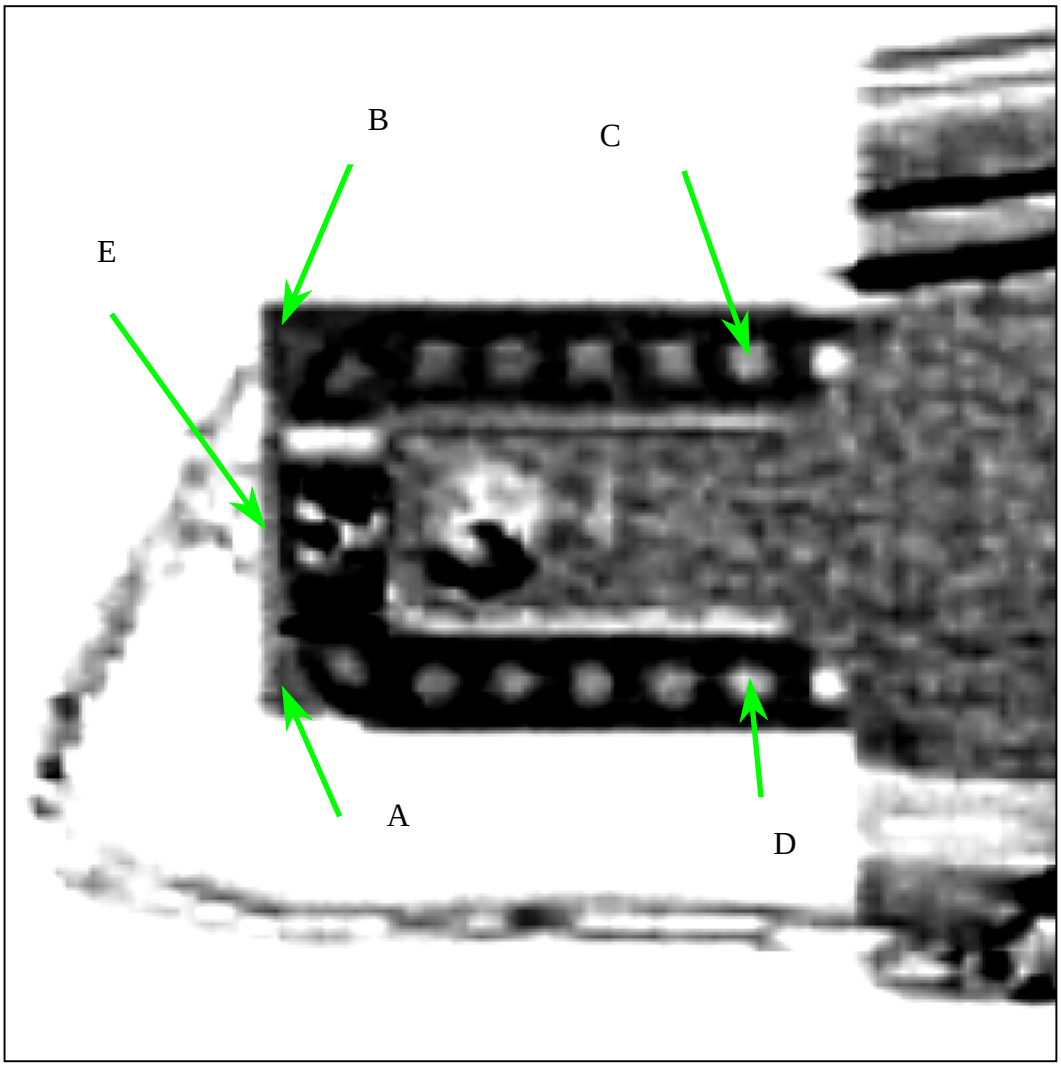

Figure 3 Suspension assembly and measurement points - Type A

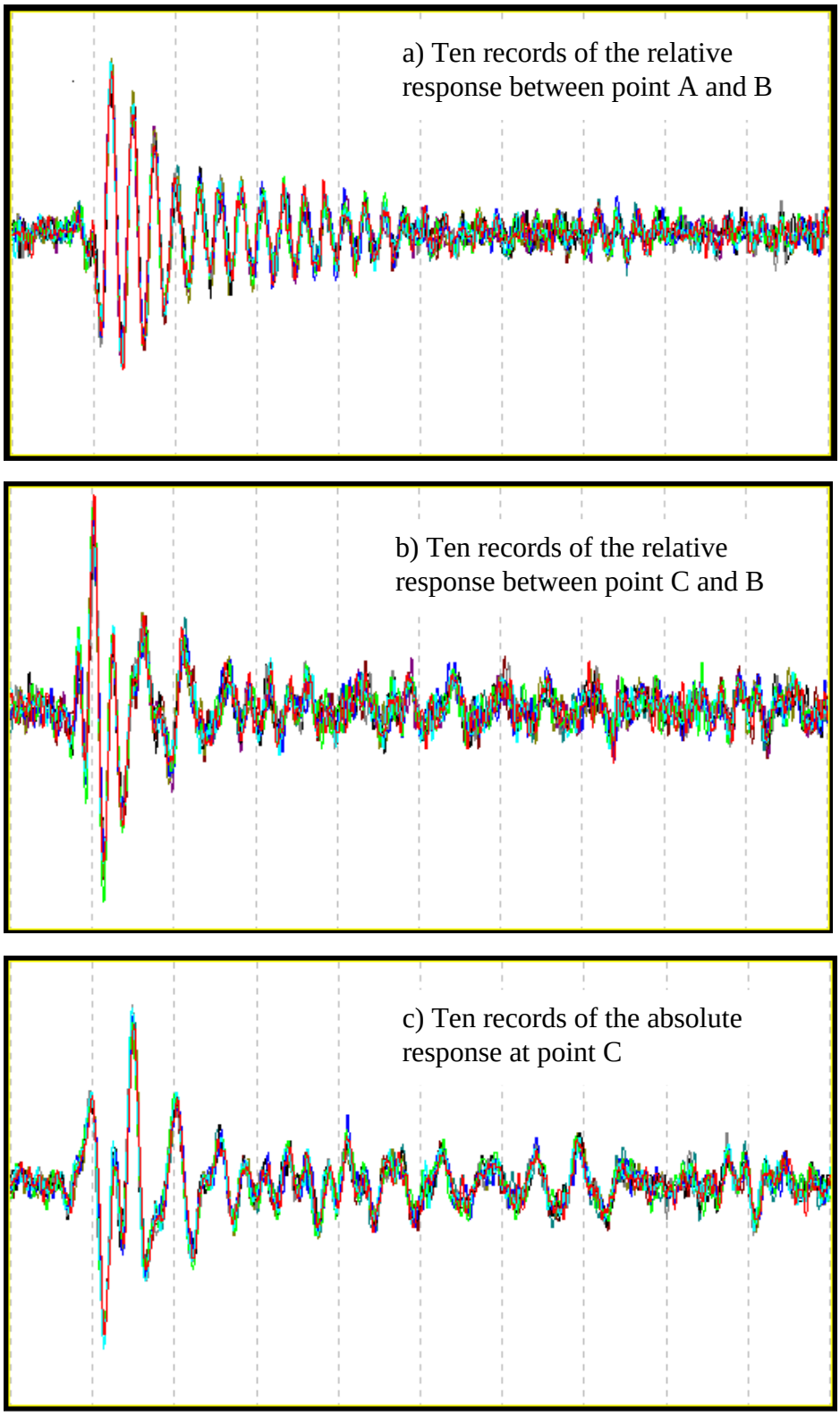

Figure 4 Measurement data – Type A

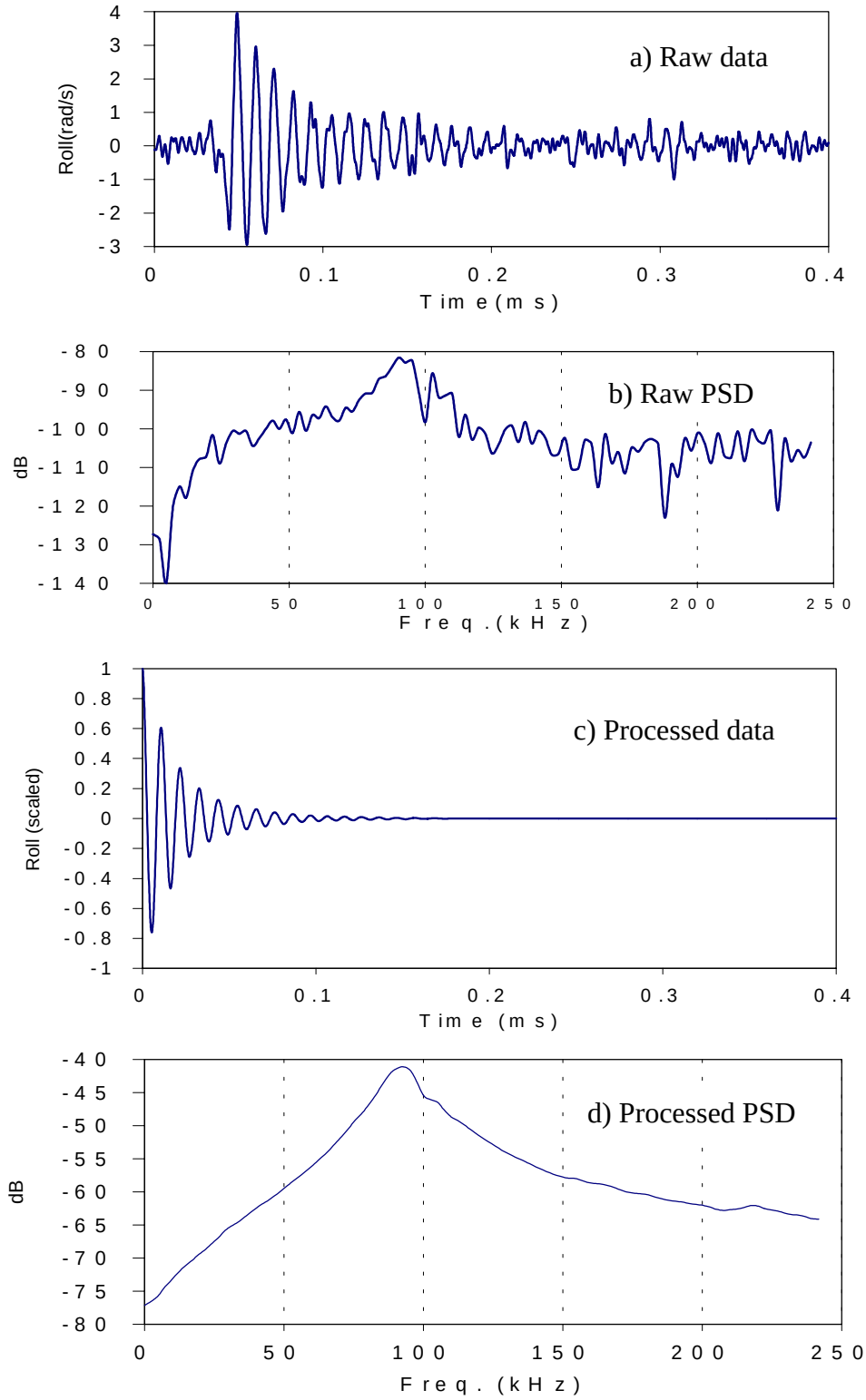

Figure 5 Measured roll response between point A and B – Type A

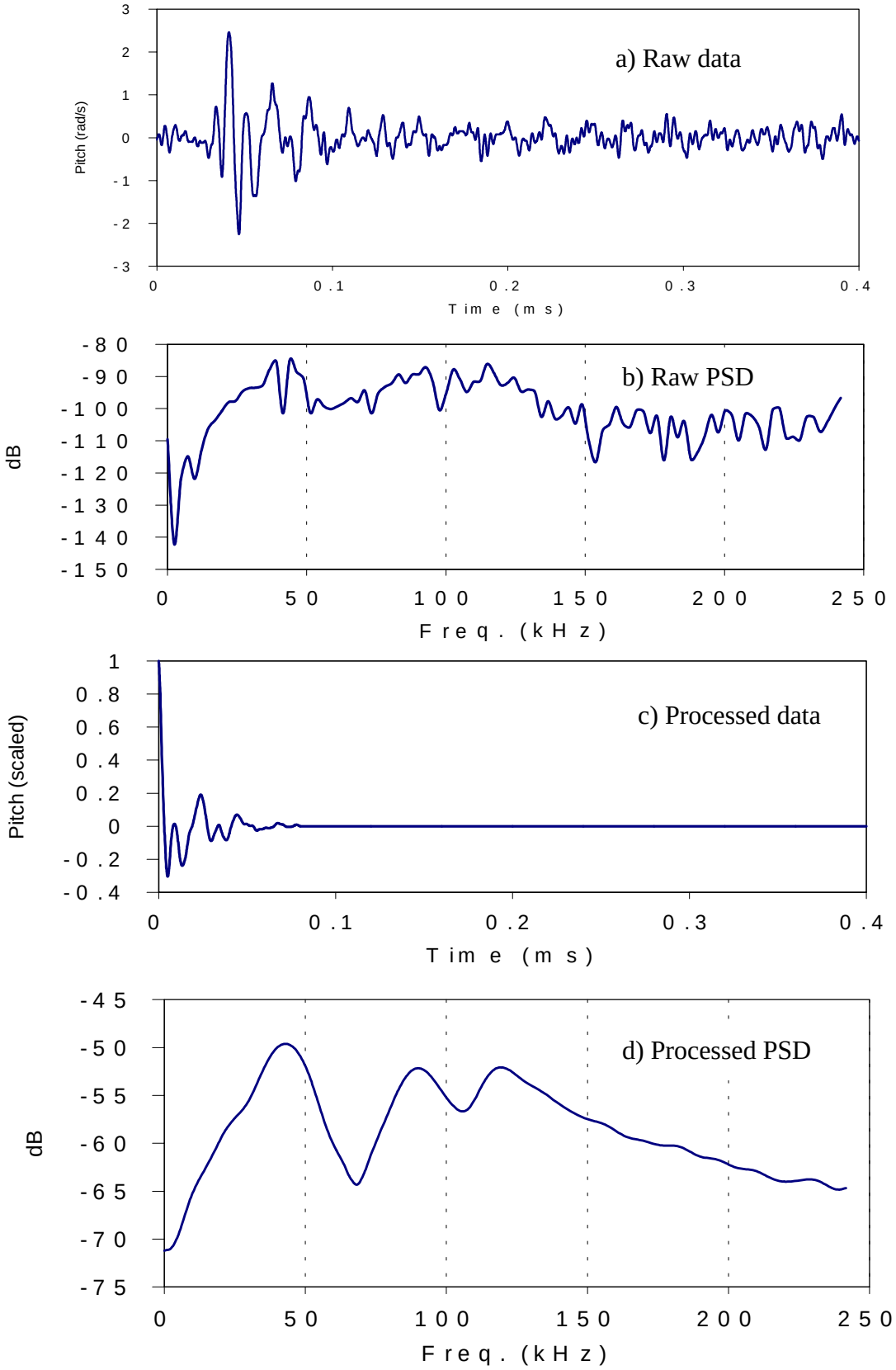

Figure 6 Measured pitch response between point C and B – Type A

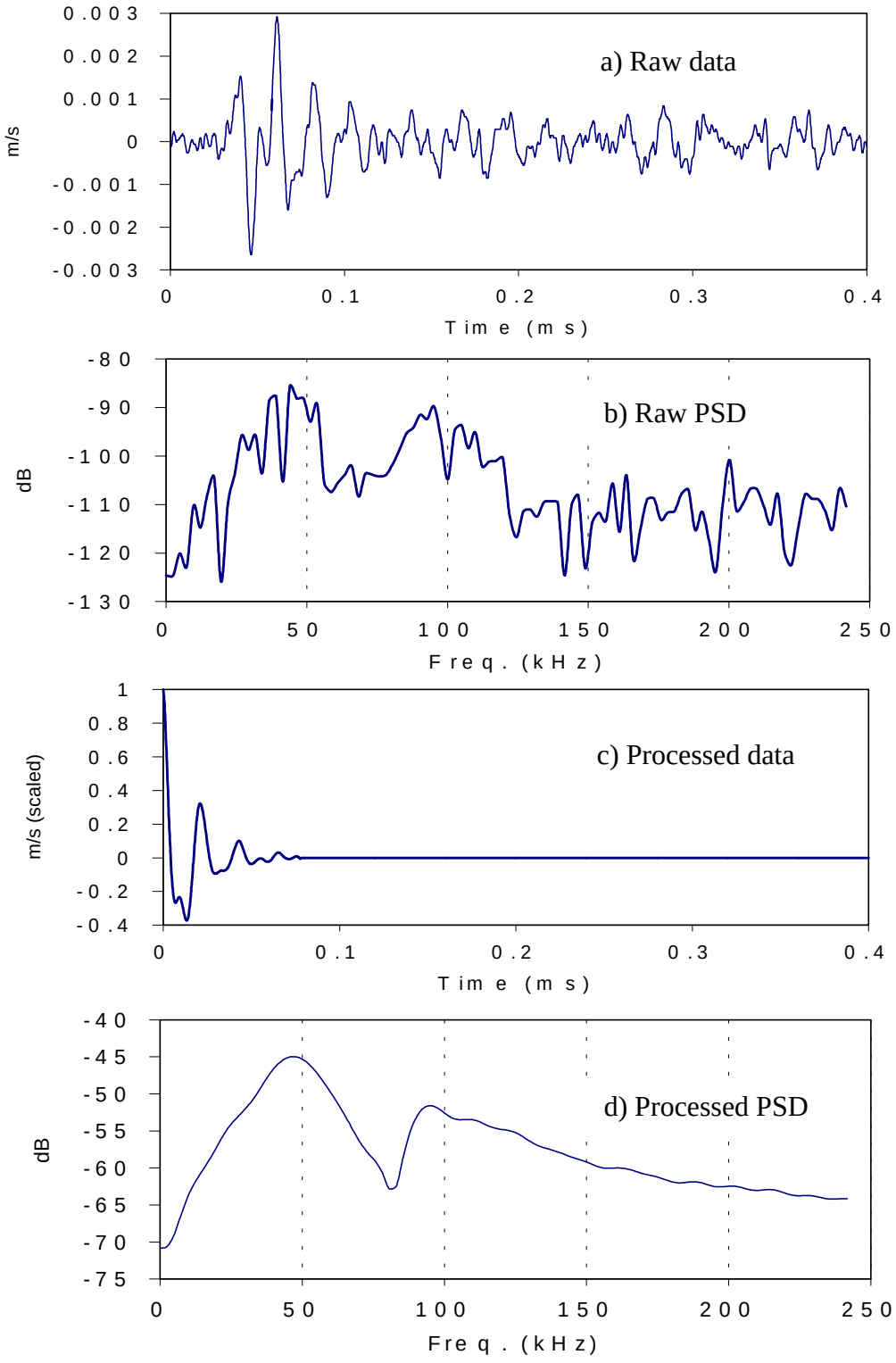

Figure 7 Measured response at point C – Type A

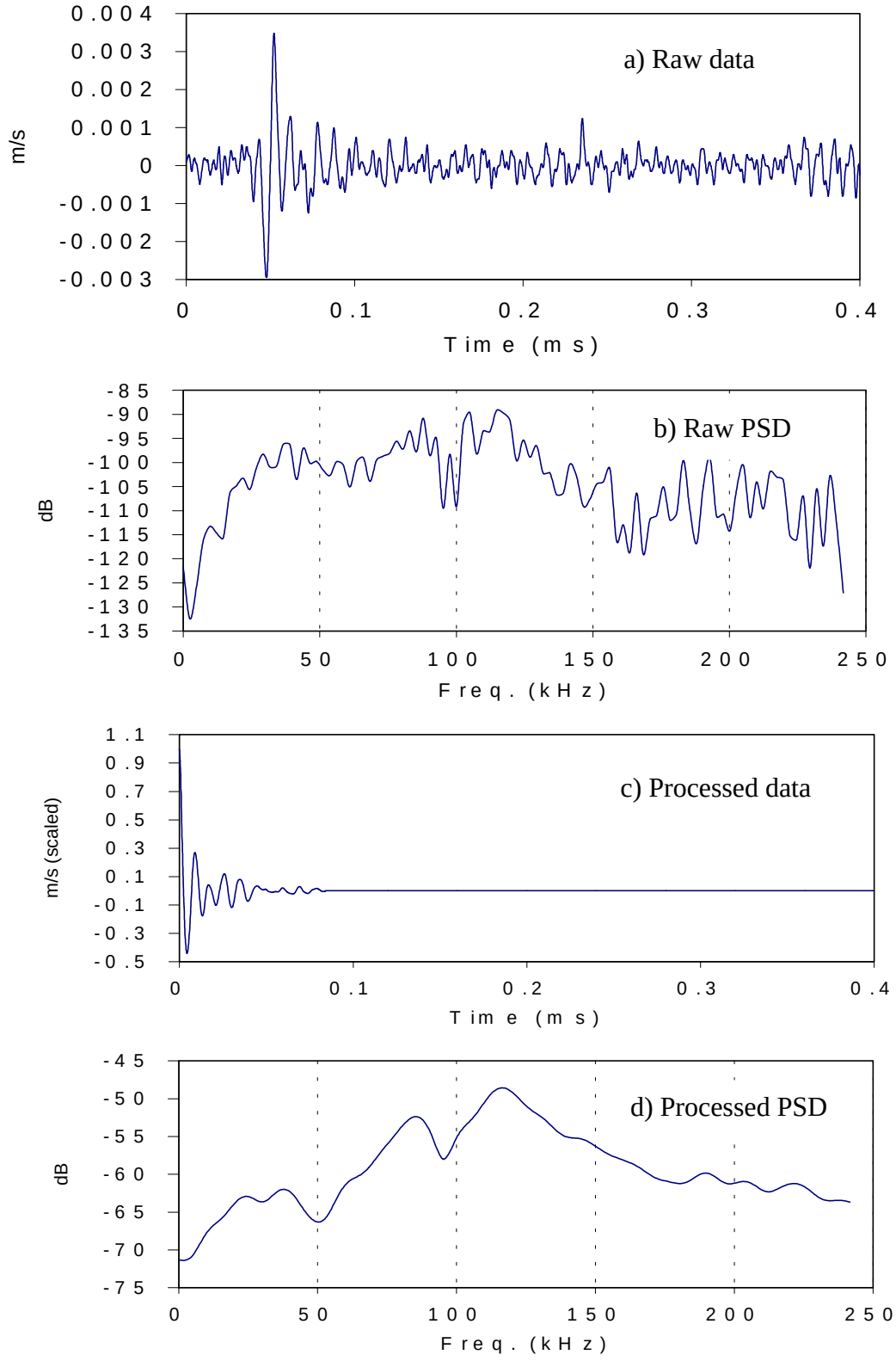

Figure 8 Measured response at point E – Type A

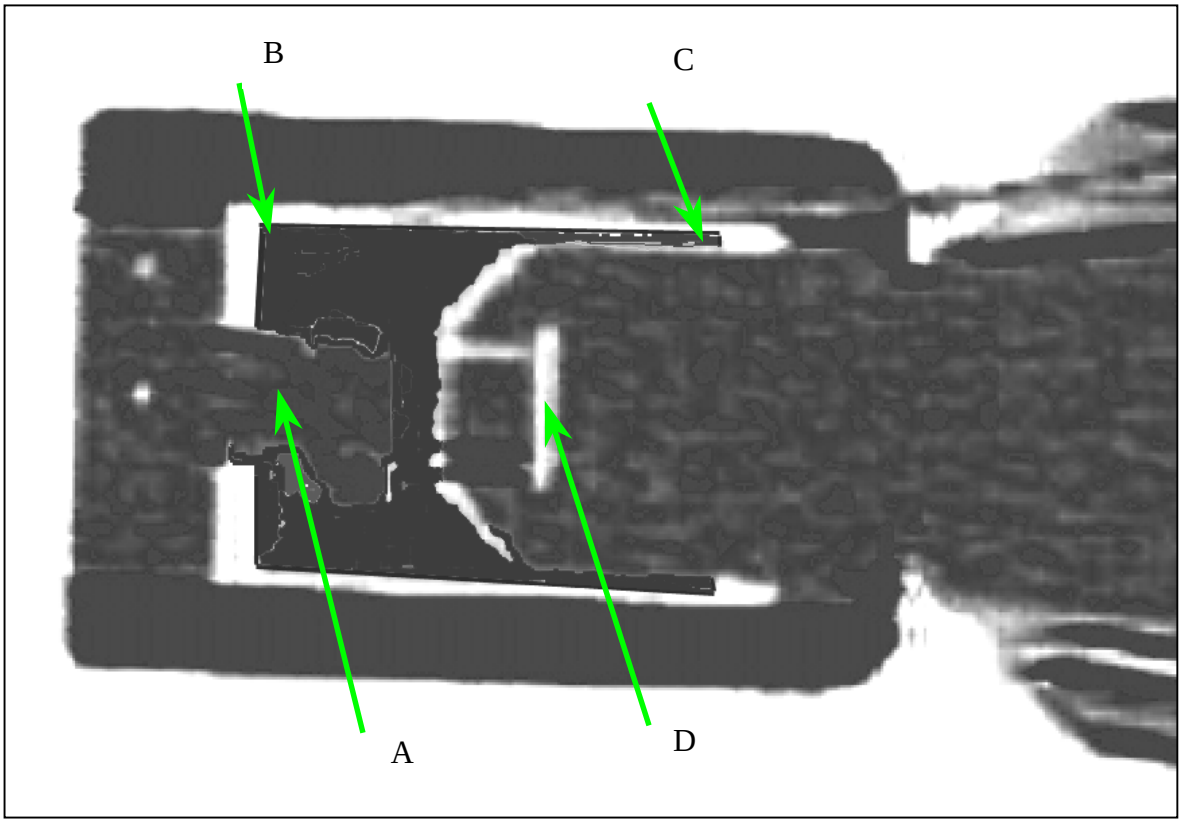

Figure 9 Suspension assembly and measurement points – Type B

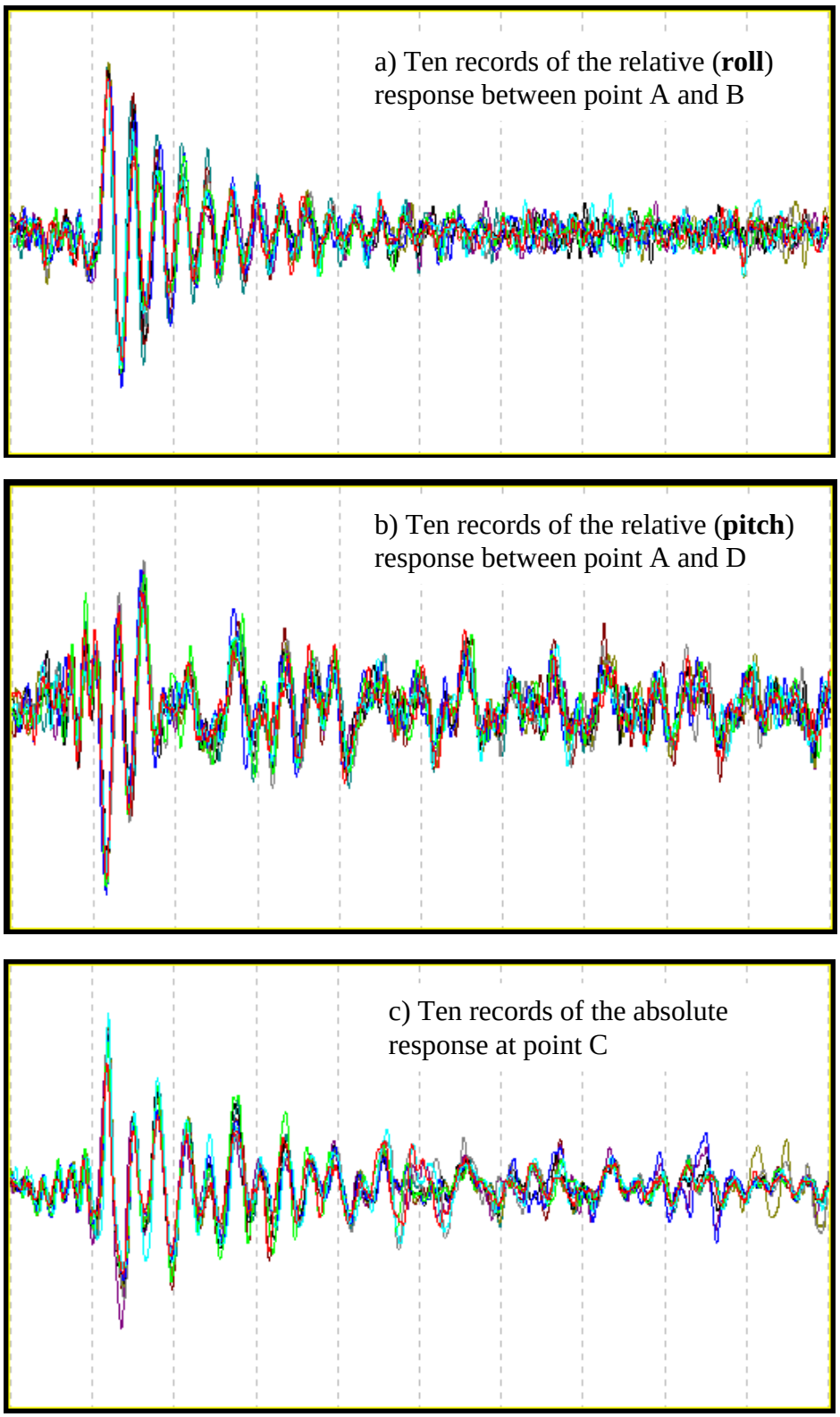

Figure 10 Measurement data – Type B

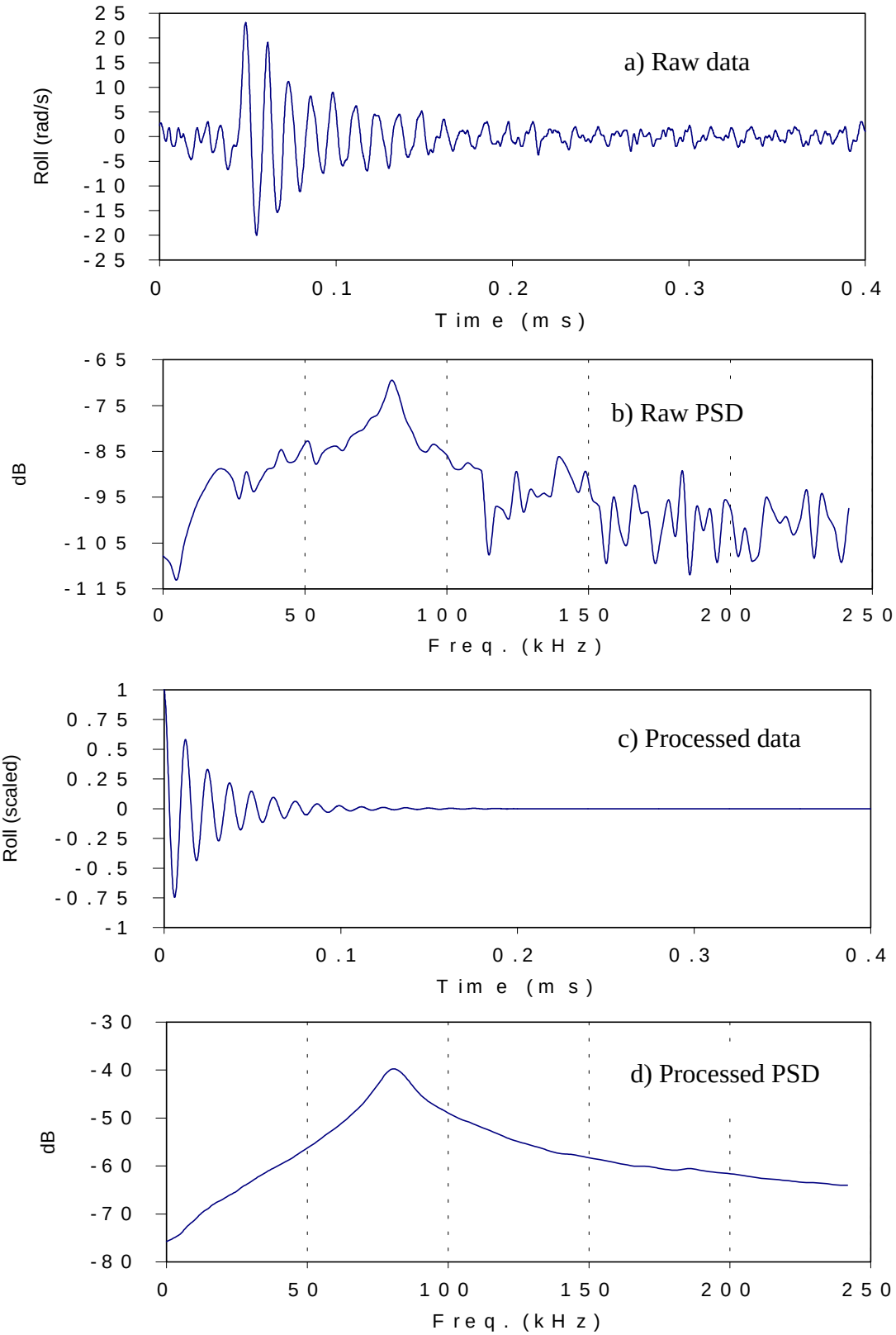

Figure 11 Measured roll response between point A and B – Type B

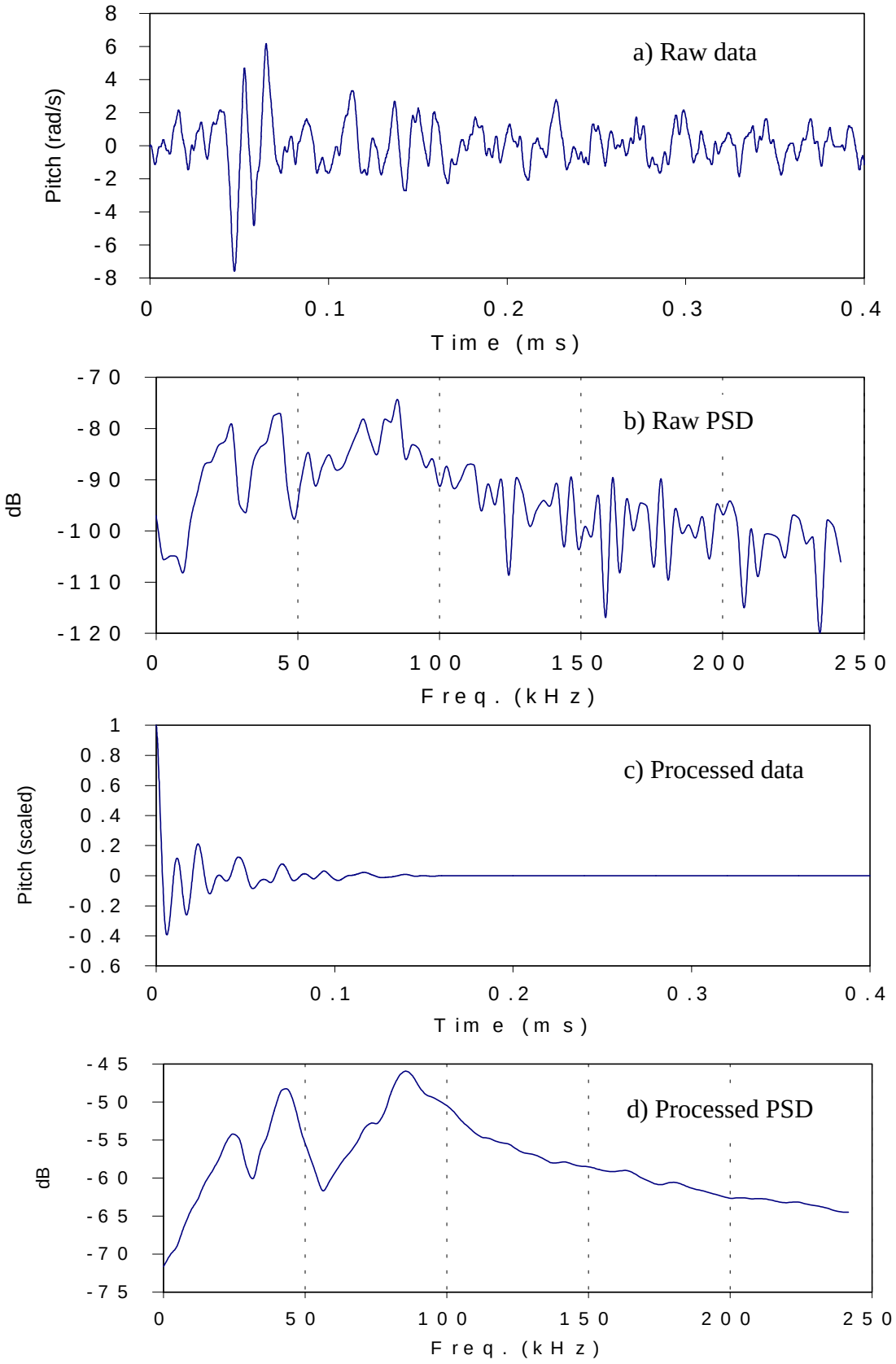

Figure 12 Measured pitch response between point A and D – Type B

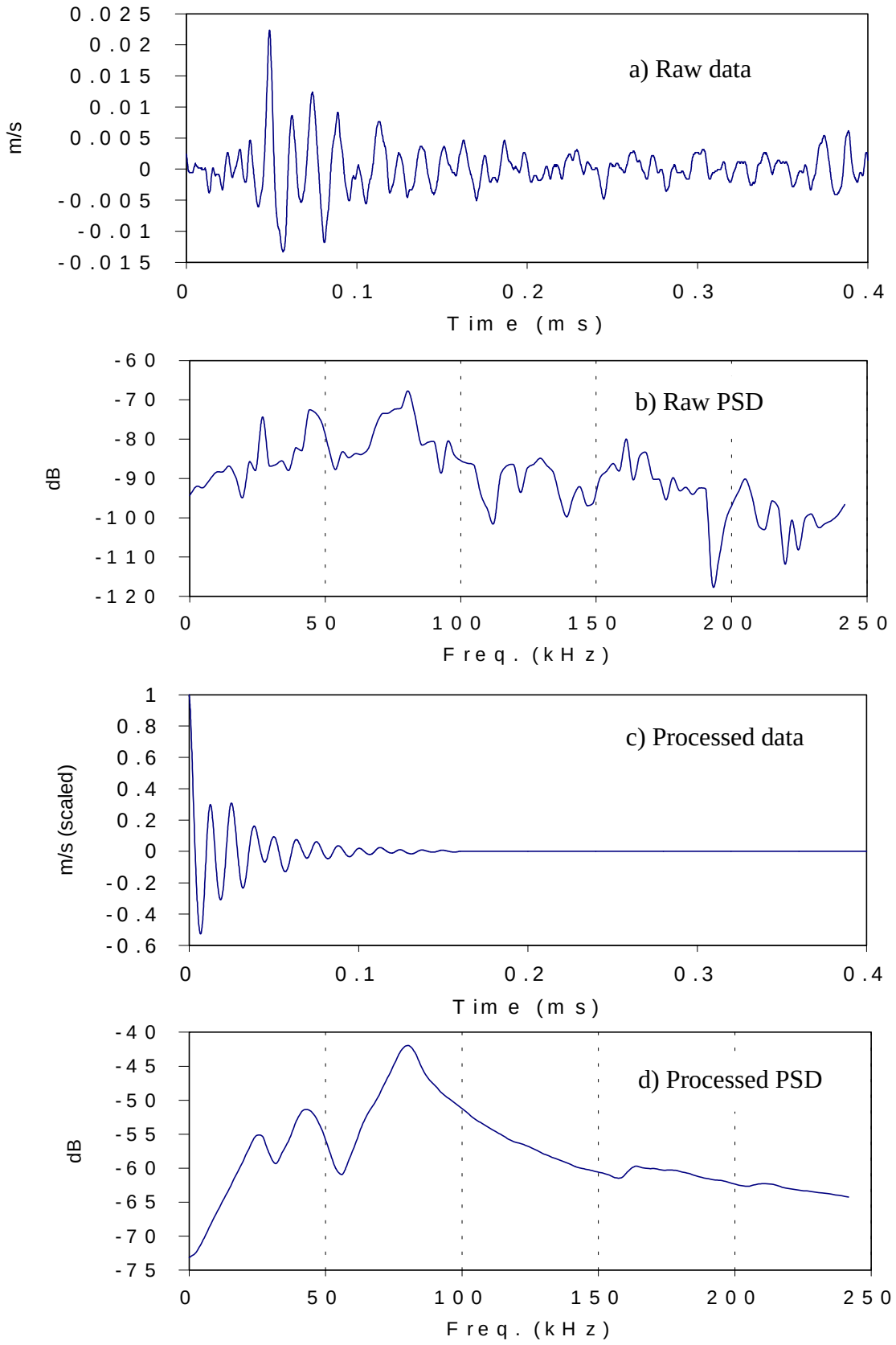

Figure 13 Measured absolute response at point C – Type B

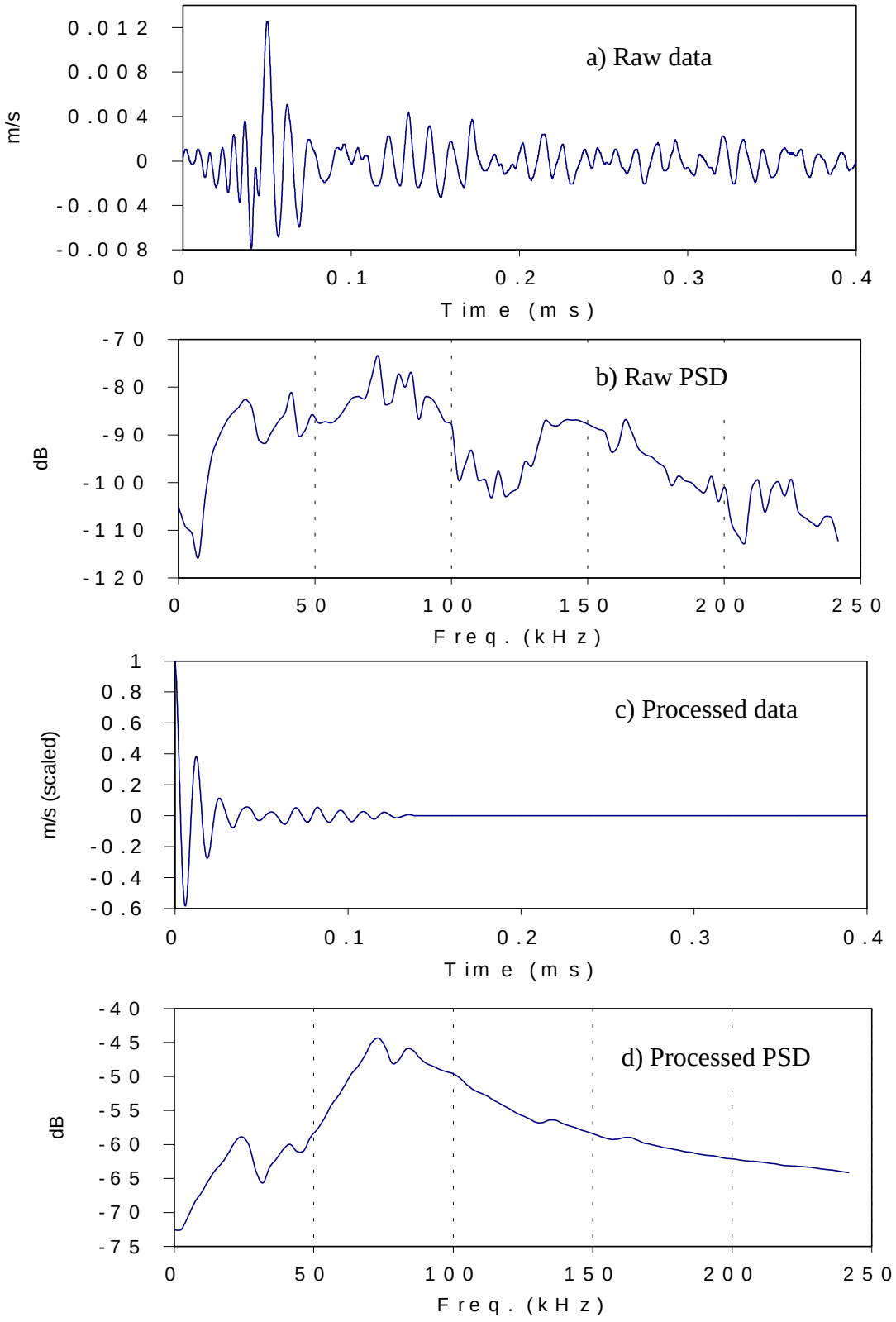

Figure 14 Measured absolute response at point A – Type B

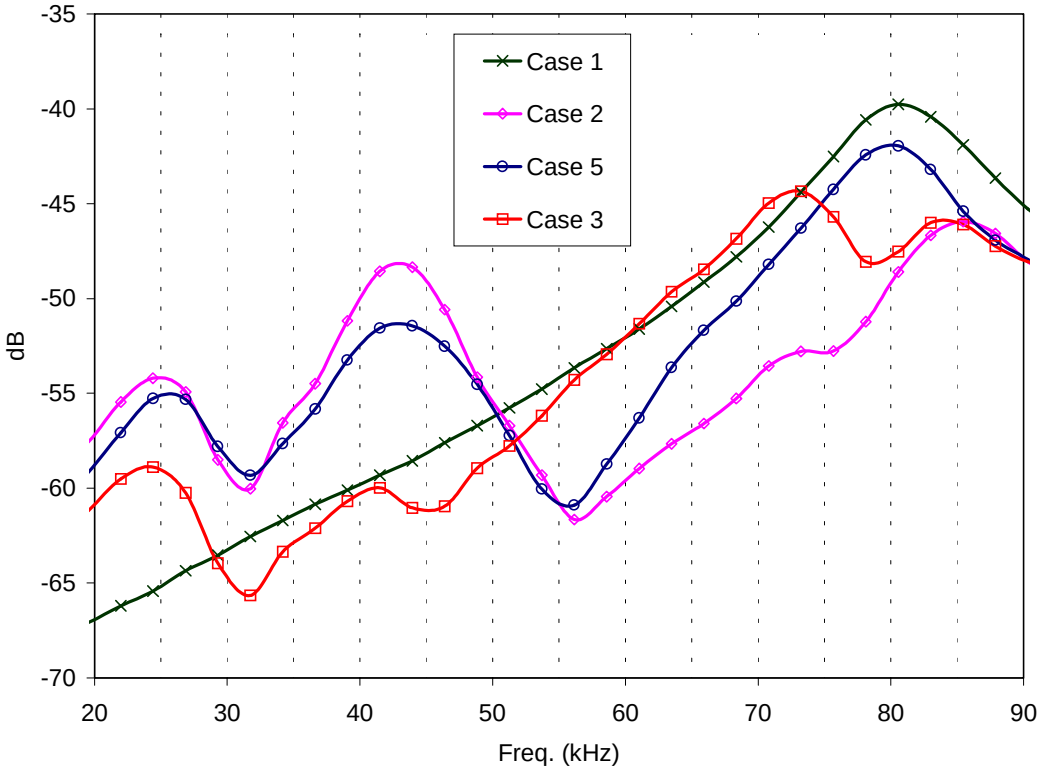

Figure 15 Comparison of the PSDs measured from different case

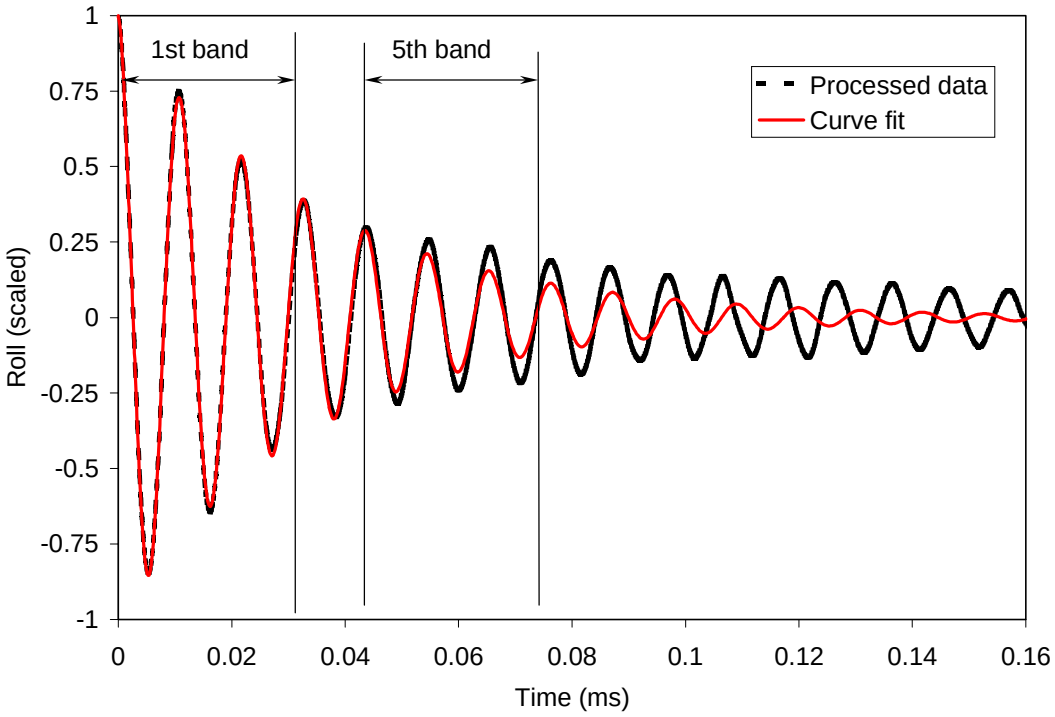

a) Type A

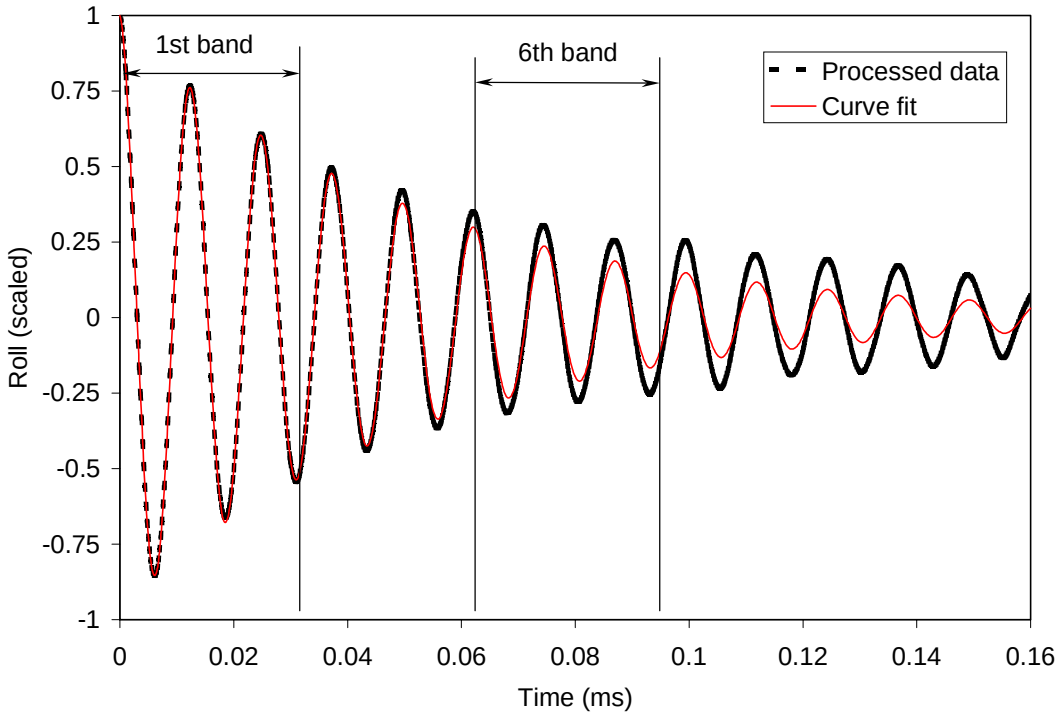

a) Type B

Figure 16 Curve fitting in the time domain – roll responses
(The width of the band used in curve fitting is fixed to .03ms. The start point of each band is located at each peak of the curves.)

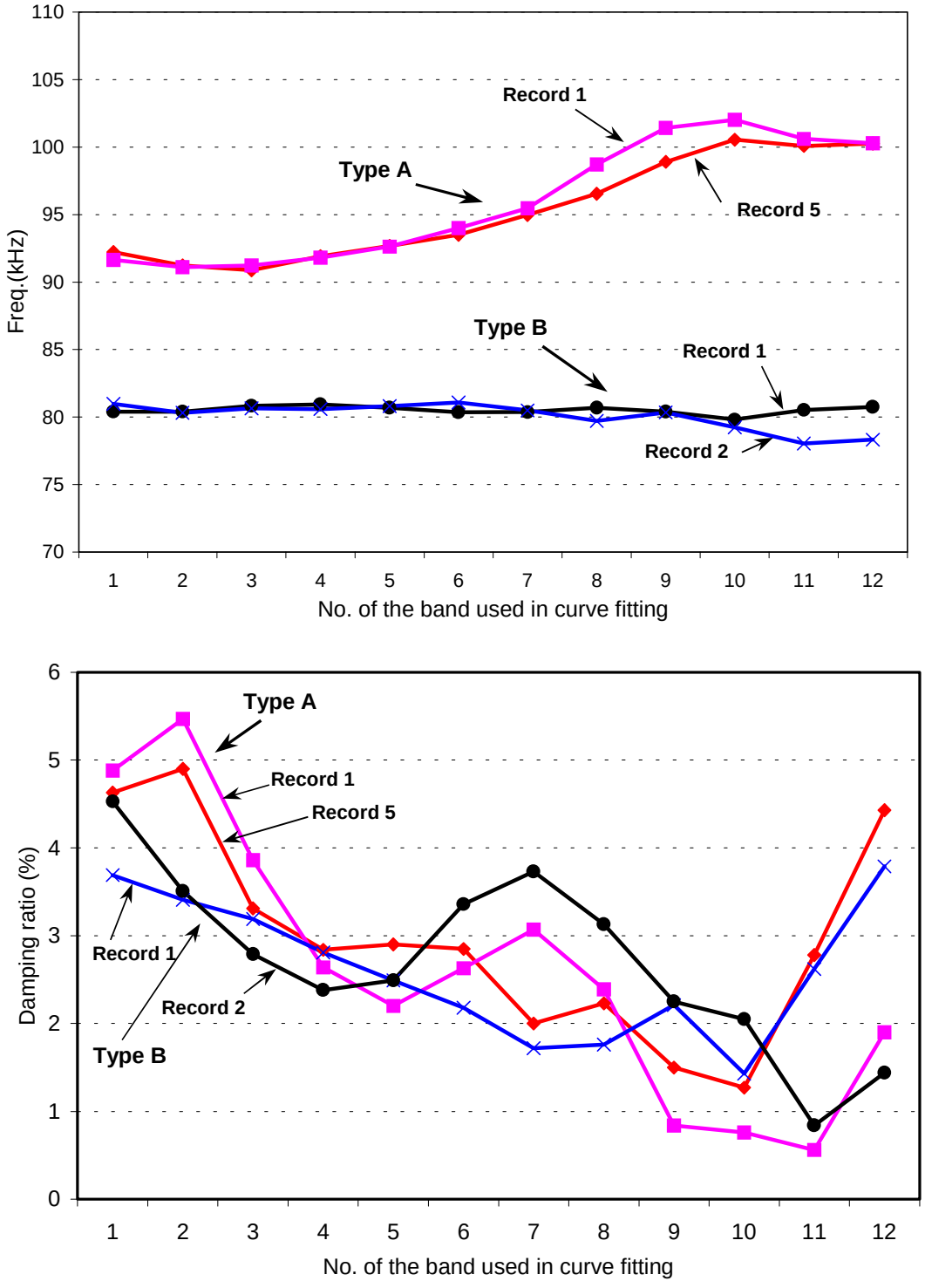

Figure 17 Modal frequencies and damping ratios of the roll mode of the two type slider (obtained from the different band by using time domain method)